Characterisation of 15 sources of Japanese obsidian: PIXE–PIGME analysis, and identification of archaeological specimens

Foss Leach,* Shizuo Oda** and Roger Bird***

* Research Associate, Museum of New Zealand Te Papa Tongarewa, PO Box 467, Wellington, New Zealand (foss.leach@gmail.com)

** University Museum the University of Tokyo, Japan

*** Formerly, Australian Atomic Energy Commission Research Establishment, Private Mailbag, Sutherland, NSW 2232, Australia

** University Museum the University of Tokyo, Japan

*** Formerly, Australian Atomic Energy Commission Research Establishment, Private Mailbag, Sutherland, NSW 2232, Australia

ABSTRACT: Samples of obsidian from 15 different volcanic sources in Kyushu, Honshu and Hokkaido were subjected to analysis using the PIXE–PIGME method. Eighteen elements were resolved for each source, and a series of statistical techniques was used to assess the distinctiveness of the sources. It was found that the sources could be separated into three groups, each with sub-sources that are virtually indistinguishable from each other. The first group of four sources originates in the Shinshu area, the second group of two sources is from the Izu Islands, and the third group contains two sources on Kyushu. Each of these groups is easily distinguished from the others. Finally, nine obsidian artefacts from three archaeological sites were analysed and compared with these sources. Eight of these could be allocated to a source, while one proved to be from an unknown source.

KEYWORDS: Obsidian, Japan, PIXE, PIGME, archaeology, source characterisation.

Introduction

Obsidian is a form of volcanic glass that can readily be flaked into tools with extremely sharp edges. It is found widely across the Pacific, as well as elsewhere in the world, and was used by prehistoric people as cutting implements. There are thought to be at least 80 sources of obsidian of varying quality throughout the islands of Japan. In this study we focused on 15 sources: eight from Honshu, two from the Izu Islands, three from Kyushu and two from Hokkaido. This represents a suitable sample of the range of geochemical variation that might be encountered when trying to identify archaeological specimens.

The main purpose of the study was to examine the range of variation of element concentrations from one source to another to see how clearly they can be distinguished. Characterisation of obsidian sources is the first step before attempting to identify the origin of archaeological specimens. As Kuzmin has pointed out (2012: 1), it may be impossible to distinguish between some primary sources of obsidian unless a wide range of elements is determined, using such methods as neutron activation analysis (NAA) and laser ablation inductively coupled plasma mass spectrometry (LA-ICP-MS). However, it is sensible to use a broad-brush strategy over the range of variation involved first, to narrow down sources that are difficult to distinguish other than by using more expensive techniques.

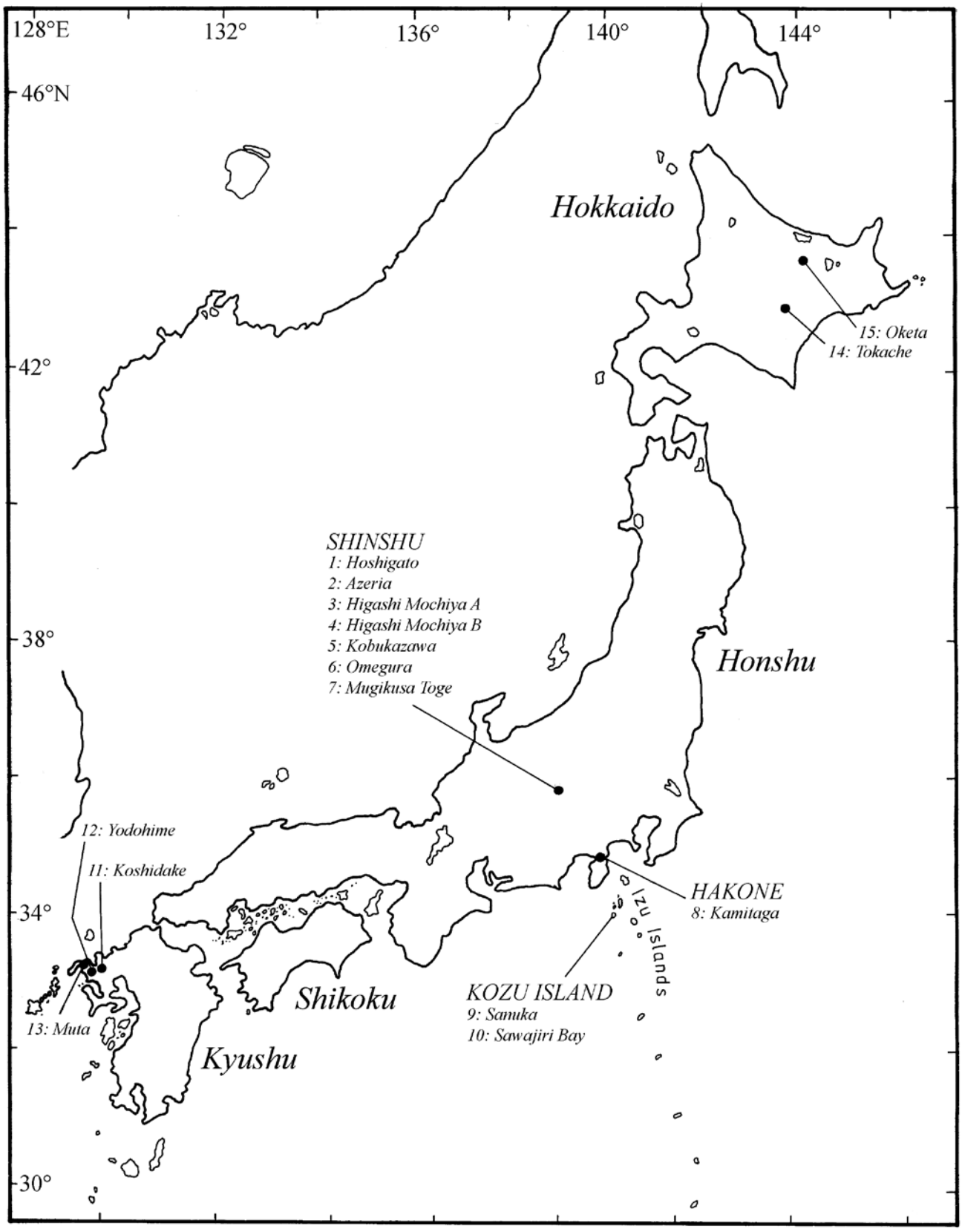

Fig. 1 Map of Japan showing the location of the obsidian sources analysed.

The volcanic sources sampled

The location of each obsidian source is shown in Figure 1. They are enumerated below. The numeral in brackets is the number of specimens analysed from each source (total=82).

Honshu

1 Hoshigatō, Shinshu Area (5).

2 Azeria, Shinshu Area (4).

3 Higashi Mochiya A, Shinshu Area (6).

4 Higashi Mochiya B, Shinshu Area (6).

5 Kobukazawa, Shinshu Area (5).

6 Omegura, Shinshu Area (5).

7 Mugikusa Toge, Shinshu Area (7).

8 Kamitaga, Hakone Region (4).

Izu Islands

9 Sanuka, Kōzu Island (6).

10 Sawajiri Bay, Kōzu Island (5).

Additional specimens from Nagahama and Onbase in the Izu Islands are very poor quality, crystalline and have many inclusions, and were not analysed.

Kyushu

11 Koshidake, Saga Prefecture (6).

12 Yodohime, Sasebo City, Nagasaki Prefecture (6).

13 Muta, Nagasaki Prefecture (5).

Hokkaido

14 Tokachi (6).

15 Oketo (6).

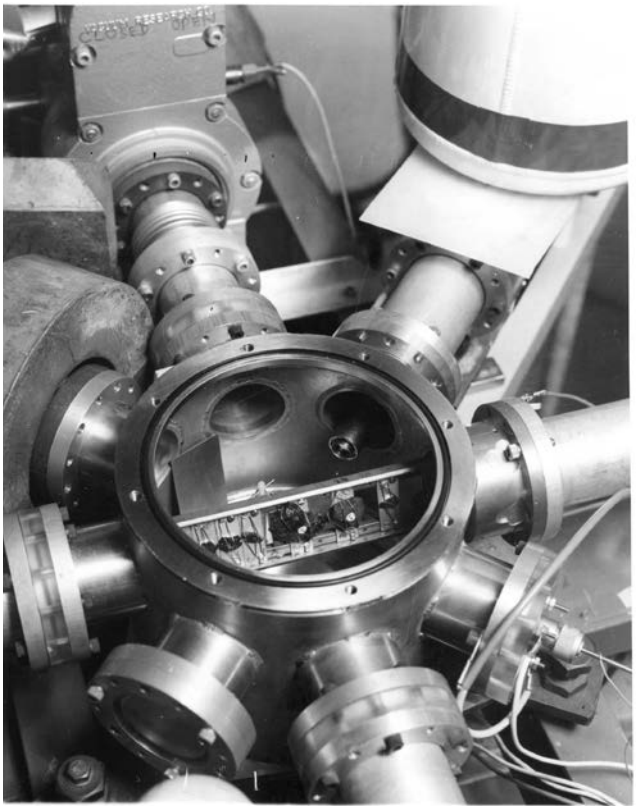

Fig. 2 The sample chamber for the PIXE–PIGME analysis of obsidian objects.

The PIXE–PIGME analytical method

The PIXE (proton induced X-ray emission) and PIGME (proton induced γ-ray emission) analytical techniques have been outlined in previous publications: the PIXE method by Duerden *et al.* (1979) and the PIGME method by Bird *et al.* (1978). The use of the joint PIXE–PIGME technique for elemental concentration measurements has been described by Duerden *et al.* (1980). The experimental arrangement for obsidian specimens ready to be analysed in this study is shown in Fig. 2.

The γ-ray and X-ray spectra collected were automatically recorded. Batches of spectra were later reduced interactively on a computer with the aid of graphics. With the use of suitable standards, absolute concentrations were determined.

A beam of 100–200 μ A of 2.5 MeV protons was used to irradiate each obsidian sample and μ-ray and X-ray detectors measured the radiation emitted during irradiation. A typical running time was five minutes per sample. Samples were pre-mounted onto target holders and these, in turn, were located by pegs on a target stick (Fig. 3), where they were held in place by magnetic

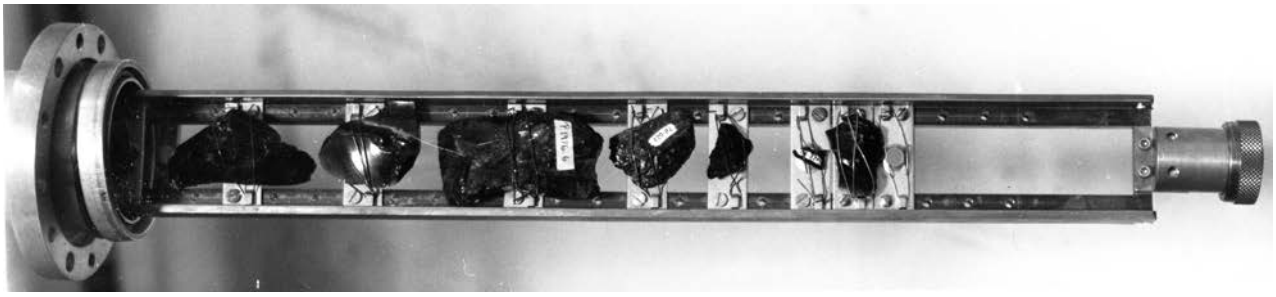

Fig. 3 Up to 60 obsidian samples at a time were mounted on a special target stick, which was then inserted into the sample chamber for analysis.

tape. The smoothest face of the sample was selected to be irradiated.

The samples were pre-cleaned and the entire loaded target stick washed by ultrasonic agitation in nanograde benzene. Although surface irregularities were minimised by cleaning, the objects were often irregular and sometimes had rough faces. The effect of roughness has been monitored statistically and has generally been found to have minimal effect (Bird *et al.* 1978). The only limitation was that the objects selected had to fit into the side tubes of the target changer. A maximum of 60 samples can be loaded onto the target stick and, with automatic sequencing, up to 200 or 300 samples can be studied per day.

The detectors were placed at 135 degrees to the direction of the proton beam. The 120 cm^3 Ge(Li) detector used for detection of the γ-rays had a resolution of 2.3 keV at 1.33 MeV and an efficiency of 1.9 x 10^4 peak counts per γ-ray for a source of the energy placed at 25 cm. The 12

Fig. 4 PIGME spectrum of an obsidian sample.

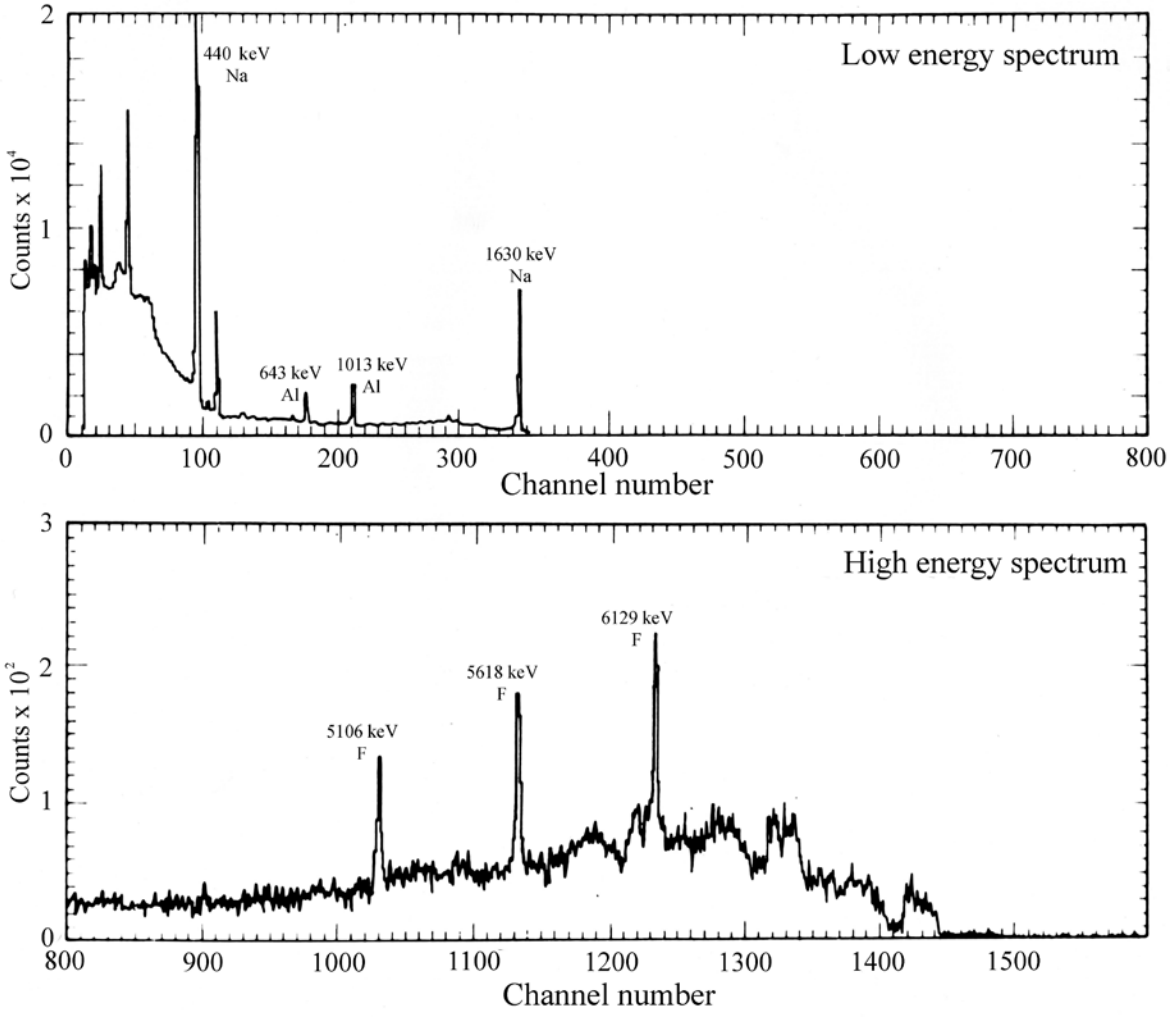

mm^2 Si(Li) detector with 4 mm depletion depth for X-ray detection was mounted via a sliding seal on a chamber port. Its resolution was 140 eV at the Mn Kσ 5.9 keV line. The efficiency of the Si(Li) detector with and without filters was measured and the efficiency functions determined.

A heated graphite filament was used to discharge any charging that could result from the proton irradiation of an insulated target, which would otherwise affect the X-ray background. The target chamber was used as a Faraday cup for collection of target current, a technique that is not completely satisfactory and that can certainly be affected by the electron flood current. A shift in absolute concentration values was seen in a limited number of repeated measurements.

A typical γ-ray spectrum from an obsidian sample is shown in Fig. 4. It can be seen that γ-rays from Na, Al and F dominate the spectrum and, although in some particular cases other γ-rays may be measured with reasonable precision, only the X-rays from the three elements (Na, Al, F) are measured on a routine basis for obsidian.

The detected X-ray spectrum is dominated by K X-rays[1] from the major elements (typically Al, Si, K, Ca, Ti, Fe), whose energies are in the range 1.5–7.0 keV. K X-rays from Zn, Pb, Sr, Y, Zr and Nb elements that appear to be significant for sourcing obsidian are many orders of magnitude lower than the previously mentioned elements and cannot be measured simultaneously without the use of a special filter. A 1 mm graphite filter was used, with a 75 μm hole laser-drilled at the centre. This allows low-energy X-rays (<6 keV) to be observed with approximately 0.1% of their normal intensity at the same time as the higher-energy X-rays, which are little affected by the filter. The resulting spectrum is shown in Fig. 5.

The detected γ-ray and X-ray spectra were analysed in part by simple data reduction during the experiment. For the γ-ray spectrum, counts of the Na 440 keV and 1630 keV peaks, the Al 643 keV and 1013 keV peaks, and the three higher-energy peaks of F were derived and stored on file. The X-ray data were reduced to 24 summations of counts between fixed energy equivalent 'windows' set

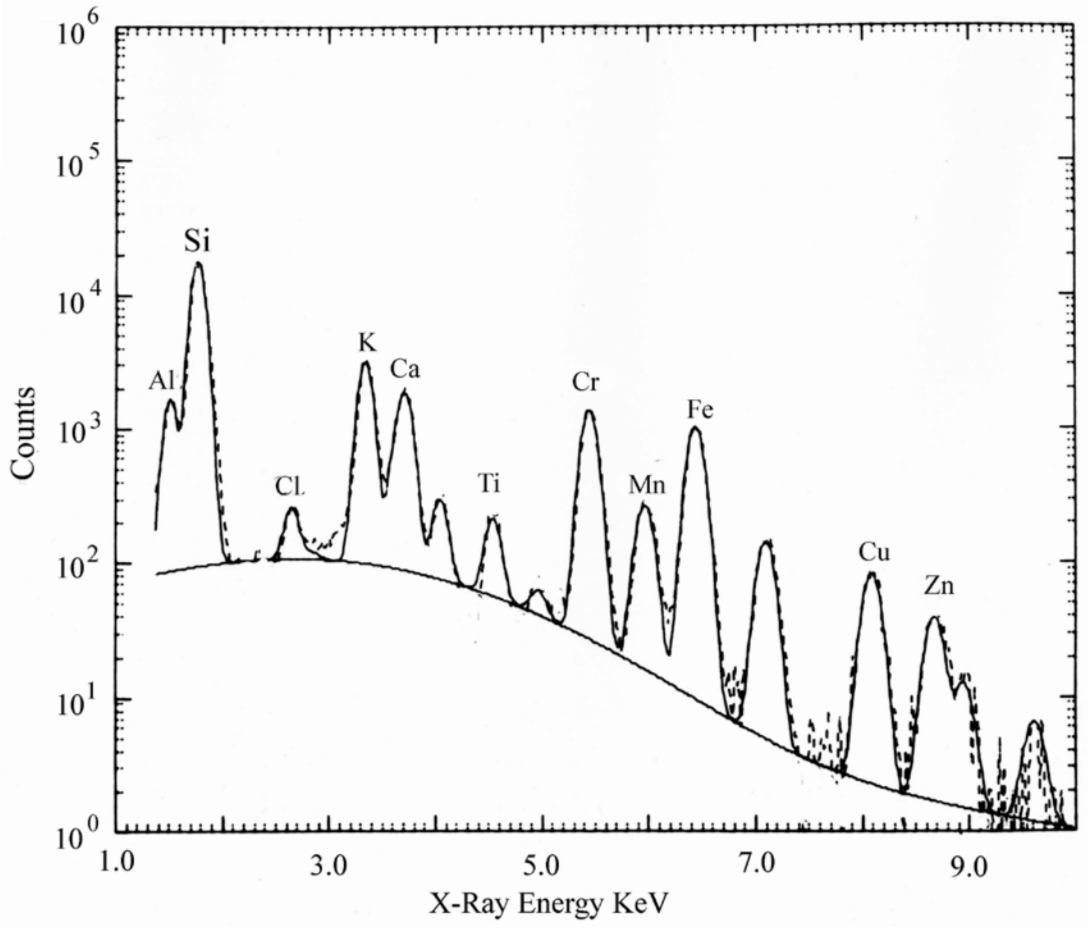

Fig. 5 (left) PIXE spectrum at 1–10 keV of a piece of obsidian. The dashed line is the experimental data, and the solid line is the analysed best fit to the data and the background component.

about prominent peaks in the spectrum. These figures were also stored on file, together with run information: sample number, run number, current, elapsed time for the counting period, etc. The complete X-ray spectrum was then stored for a more complete analysis offline.

This analytical procedure has been described in detail by Clayton (1982a,b), and essentially consists of fitting a predetermined background shape and Gaussians representing characteristic X-ray peaks to the spectra. The relative intensity and the energies of the characteristic X-rays for a particular element are fixed, but the overall magnitude of the peaks, and of the background, are scaled to best fit the data. Once again, the resulting analysed elemental data were stored on file. An example of the fit to a typical X-ray spectrum is shown in Fig. 5. It can be seen that the peak/background ratio is much higher for some elements than others. The precision of measurement within the spectra therefore varies from element to element, but can also change from spectrum to spectrum because of the relative element concentrations.

A full calculation was made for the number of X-rays detected per 100 μC per 100 μg/g of a trace element within an obsidian sample. These yield values were then used to convert all analysed data to elemental concentration either in percentage by weight or μg/g.

Precision of results

A standard overall error of ±5% is present for all concentrations listed. This primarily results from inaccuracy of current measurements. However, within an analysis, an improved accuracy can be expected in element ratios. No repeat measurements were made, but from measurements made on different rocks from the same source we can make some generalised comments about measurement precision.

The final precision is therefore suggested to be:

Gamma-ray measurements

Na ±20%; Al, F ±3%

X-ray measurements

Rb, Mn, Fe ±5%; K ±6%; Si, Ca ±7%; Sr ±8%; Zr ±9%; Ga ±12%; Ti ±20%; As, Pb, Br, Zn ±30%; Y and Cu usually low concentration, so poor precision ±~50%

Element results for source samples

A total of 82 obsidian samples from the 15 sources were analysed. Each sample was allocated a catalogue number beginning with two letters (JD, JE, etc.), so that individual items can be referred to. The Japan samples were part of a larger run that included an additional 567 samples from other parts of the Pacific region (see Fig. 6 and Duerden *et al.* 1987).

The obsidian samples from two additional sources from Nagahama and Onbase in the Izu Islands were of such a low quality that no valid measurement could be made with our analysis technique. The element concentrations for samples from a source were generally in agreement with one another within the errors of the measurement technique. There were, however, three anomalous results:

1 Higashi Mochiya A, sample JD405. Most element concentrations are in agreement with other JD samples, but Ca is 1.12%, whereas for other samples the average Ca is 0.46±0.02, and Sr is 108 μg/g, compared with 17±7 μg/g for other samples from the same source.

2 Higashi Mochiya B, sample JE503. Most elements are in agreement with other JE samples, but Zr is 216 μg/g, compared with 83±4 μg/g for other samples.

3 Higashi Mochiya B, sample JE508. The values for Ti, Fe and Sr for this sample appear to be very different to others from the same source.

Table 1 Mean element concentrations for the 15 Japanese obsidian sources sampled (Fig. 1). Note that the mean is listed as zero for source 8 as no value was determined.

Source	Major elements (%)						Minor elements (μg/g)											
	Na	Al	Si	K	Ca	Fe	F	Ti	Mn	Zn	Ga	As	Pb	Rb	Sr	Y	Zr	Nb
1	2.55	6.14	37.72	3.86	0.41	0.58	663.1	679.0	810.1	26.4	13.3	14.5	4.7	149.0	42.0	18.8	75.9	3.7
2	2.68	6.39	38.78	3.97	0.41	0.64	1140.7	424.4	1162.9	28.0	24.0	15.8	4.4	315.6	6.6	24.0	94.5	7.1
3	2.56	6.23	35.40	3.59	0.57	0.67	1021.1	673.8	1023.5	25.4	19.0	16.0	1.4	277.5	17.0	23.1	80.3	9.3
4	2.55	6.27	36.62	3.66	0.53	0.79	1046.2	458.5	1064.4	21.1	18.1	19.0	2.1	279.1	13.7	27.2	104.9	5.6
5	2.67	6.36	40.36	4.00	0.47	0.67	1111.7	617.3	1155.3	26.3	21.9	24.6	4.0	305.3	10.4	22.4	83.4	5.9
6	2.53	6.24	36.74	3.70	0.58	0.84	556.9	1235.0	765.1	21.8	10.4	12.3	5.1	163.8	82.8	11.6	127.7	2.5
7	2.64	6.36	36.24	3.17	0.64	0.88	596.2	1412.1	573.5	17.9	9.4	17.4	6.0	101.0	136.8	16.7	114.6	3.7
8	3.11	6.30	36.89	1.37	1.29	1.45	379.6	1288.9	579.0	16.7	8.5	7.3	3.1	31.9	142.6	25.9	144.4	0.0
9	2.92	6.47	41.39	3.12	0.63	0.68	288.8	1008.1	867.9	17.1	1.9	6.7	0.6	75.4	67.7	20.9	58.7	5.5
10	2.88	6.25	38.64	2.70	0.65	0.72	273.9	866.2	859.1	17.7	3.7	4.8	1.0	69.5	76.9	16.4	71.6	2.9
11	2.62	6.64	39.76	4.02	0.54	1.04	557.7	345.2	524.5	25.5	13.8	21.0	2.7	204.2	43.8	8.9	61.6	14.7
12	2.83	6.88	36.29	3.47	0.76	1.33	386.0	659.6	537.5	23.3	10.6	16.8	1.7	144.3	106.1	9.2	117.2	11.1
13	2.57	6.61	37.77	3.90	0.56	1.00	557.2	443.5	481.5	22.3	12.6	20.5	2.7	201.6	46.9	10.8	83.4	11.6
14	2.47	6.20	37.69	3.31	0.70	0.97	280.0	892.6	430.9	18.1	6.7	15.7	1.6	151.7	64.9	14.1	94.7	1.4
15	2.71	6.47	38.94	3.48	0.60	0.98	428.5	545.2	519.4	21.0	7.1	18.2	1.7	160.0	56.6	21.5	76.0	1.5

Table 2 Standard deviations of element concentrations for the 15 Japanese obsidian sources sampled (Fig. 1). Note that the standard deviation is listed as zero for sources 8 (no value determined) and 9 (only one value determined).

Source	Major elements (%)						Minor elements (μg/g)											
	Na	Al	Si	K	Ca	Fe	F	Ti	Mn	Zn	Ga	As	Pb	Rb	Sr	Y	Zr	Nb
1	0.12	0.26	2.90	0.21	0.03	0.01	26.6	53.9	38.1	0.4	0.6	3.3	0.02	7.3	3.5	7.0	27.0	3.2
2	0.05	0.18	1.58	0.05	0.01	0.02	19.5	63.6	67.3	6.2	5.3	6.0	2.7	5.6	3.1	8.5	11.0	3.7
3	0.05	0.30	3.11	0.39	0.27	0.06	40.1	157.4	54.3	2.8	2.6	4.1	0.6	13.3	6.2	7.5	3.2	5.6
4	0.03	0.19	2.21	0.22	0.17	0.35	10.2	132.2	24.2	5.4	3.2	6.4	2.0	17.2	1.5	4.2	54.8	2.5
5	0.05	0.13	4.03	0.36	0.07	0.05	22.1	24.5	81.2	10.0	4.3	12.8	3.4	11.8	4.5	4.9	3.7	3.6
6	0.03	0.17	2.19	0.24	0.02	0.02	21.3	145.3	15.3	0.8	2.1	2.4	1.2	8.6	12.0	5.6	13.3	2.0
7	0.06	0.25	4.05	0.45	0.06	0.06	18.8	222.0	16.9	4.1	2.0	5.8	1.0	4.5	12.7	4.1	12.3	2.3
8	0.06	0.25	3.61	0.07	0.17	0.11	35.9	105.6	35.8	0.7	1.7	1.4	0.3	4.2	11.5	6.1	10.2	0.0
9	0.15	0.21	3.92	0.21	0.06	0.03	10.5	95.0	63.9	1.8	0.7	2.1	0.2	7.2	10.2	0.9	7.7	0.0
10	0.01	0.04	2.21	0.10	0.05	0.04	8.5	95.0	45.7	0.7	0.4	2.0	0.9	6.1	3.1	2.1	5.0	0.9
11	0.04	0.23	4.09	0.41	0.06	0.11	19.6	139.6	37.4	2.8	2.0	3.5	0.7	7.8	2.0	3.4	7.1	2.1
12	0.02	0.17	3.24	0.24	0.06	0.03	7.7	138.6	16.1	1.4	2.3	3.1	0.5	3.4	3.3	3.0	12.0	2.5
13	0.05	0.09	2.99	0.17	0.03	0.06	6.9	192.6	47.2	5.9	4.4	6.6	1.0	9.9	4.2	3.5	21.9	7.2
14	0.02	0.12	2.75	0.22	0.05	0.03	2.2	149.7	35.2	0.6	1.1	1.7	0.7	3.4	4.7	3.5	6.7	1.8
15	0.02	0.06	2.29	0.21	0.02	0.02	6.8	147.2	22.0	1.6	2.5	3.8	0.9	3.0	1.7	4.6	3.4	1.2

Comparison with other published research

Kuzmin *et al.* (2013: 361) provide useful comparative data from their NAA analysis of samples of obsidian from four sources on Hokkaido, two at Oketo, and two from the Shirataki region. Our Tokachi source material is also from the Shirataki field, but about 3.5 km southeast of the Kuzmin *et al.* sampling areas. There are nine elements in common between the NAA study by Kuzmin *et al.* and our own PIXE-PIGME analysis; the two sets of results are compared in Table 3. There is good agreement between the two analyses, although the Sr values determined by NAA seem rather low compared with those by PIXE–PIGME in the case of the Shirataki series. However, Sr is not an easy element to resolve in an obsidian matrix using NAA, and results are not very reliable (Leach 1996: 88; Leach & Warren 1981). The peak is very close to three other isotopes (^{131}Ba, ^{65}Zn, ^{85}Sr and ^{147}Nd, situated at 496 keV, 511 keV, 514 keV and 531 keV, respectively), and appears as only a small peak above background after 30 days, when long-lived isotopes are counted.

Table 3 Comparison of two studies of Hokkaido obsidians. A = PIXE–PIGME results, this study (mean values); B = NAA results from Kuzmin *et al.* 2013: 361 (mean values).

	Na	Al	K	Mn	Fe	Zn	Rb	Sr	Zr
	±20%	±3%	±6%	±5%	±5%	±30%	±5%	±8%	±9%
Tokachi/ Shirataki									
A	2.47	6.20	3.31	431	0.972	18.1	152	66	95
B	2.87	6.80	3.82	384	0.788	37.5	150	28	90
B	2.94	6.85	3.85	451	0.743	35.6	174	<15	87
Oketo									
A	2.71	6.47	3.48	519	0.982	21.0	160	57	76
B	2.77	6.55	3.46	321	0.732	27.0	135	74	116
B	3.13	6.60	2.84	371	0.900	37.0	98	89	129

The geochemical character of the obsidian

Volcanic glasses have been classified in a number of ways. For example, the weight percentage of silica is used to distinguish between three types (after Macdonald 1974: 500 ff.):

1 Rhyolitic obsidian >66 wt% SiO_2
2 Dacitic obsidian <66 >52 wt% SiO_2
3 Tachylite (basaltic glass) <52 wt% SiO_2

In addition, the agpaitic index – the molecular ratio of $(Na_2O + K_2O)/A1_2O_3$ – has proved to be a useful means of distinguishing between:

4 Peralkaline obsidian >1.00 agpaitic index
5 Alkaline or calc-alkaline <1.00 agpaitic index

The so-called mildly peralkaline obsidians (comendites) have an agpaitic index of between 1.00 and 2.50. Finally, it should be noted that the agpaitic index has also been used (by Smith *et al.* 1977) to distinguish between oceanic obsidians from diverging or tensional (extensional) plate boundaries, and circum-oceanic obsidians from converging or compressional (subducting) plate boundaries:

6 Oceanic obsidians >1.00 agpaitic index
7 Circum-oceanic obsidians <1.00 agpaitic index

The data in Table 1 were used to calculate these molecular ratios. The results are plotted in Fig. 6, together with other data from Pacific Island obsidians (Leach *et al.* 1986). It can be seen that, with the exception of three marginal pieces, the Japanese obsidian is clearly classed as rhyolitic and alkaline, and belongs to the circum-oceanic group. The three items that are slightly to the left of the dacitic/rhyolitic boundary are one piece from Higashi Mochiya A, one from Mugisaka and one from Yodohime.

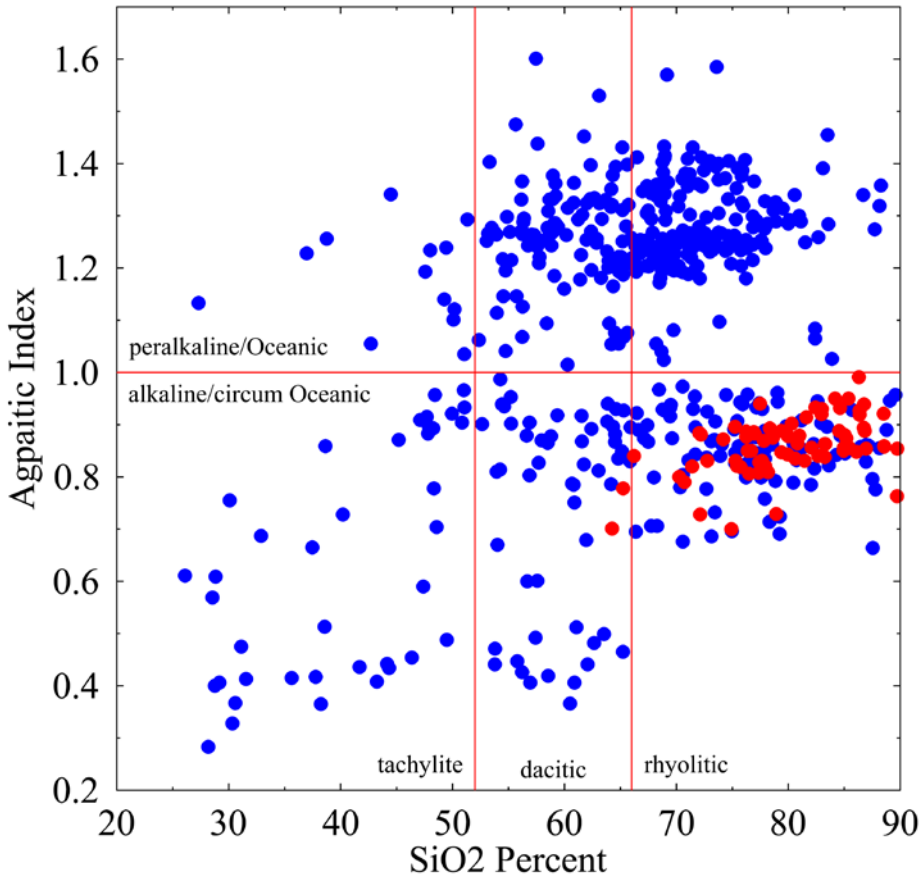

Fig. 6 Classification of Japanese and other Pacific obsidian samples. The obsidian samples from Japanese sources are shown in red, while the blue dots indicate other obsidian samples from elsewhere in the Pacific region.

Discrimination between the 15 sources

The different elements resolved through any method of analysis do not have equal power to discriminate between different sources. One obvious reason is that the concentration of any one element may vary so much from one specimen to another that the different sources appear similar. A less obvious reason is that the concentration of some elements can be highly correlated with others, so the additional elements do not add new information when trying to discriminate between sources. There are several such cases of high correlation among these sources of obsidian from Japan. These are listed below ($r > 0.6$):

K/Si	0.97
Mn/K	0.92
Al/Na	0.90
Mn/Si	0.90
Ca/Al	0.85
Fe/Ca	0.85
Rb/F	0.85
Fe/Al	0.83
Ca/Na	0.73
Fe/Na	0.67

Such correlations vary from one source of obsidian to another, thus negating one of the important assumptions involved in many statistical techniques commonly used when assessing similarity and dissimilarity between groups of multivariate data, that is a uniform variance–covariance matrix. Linear discriminant function analysis is therefore invalidated. This problem was addressed by Leach and Manly (1982), and a minimum Mahalanobis distance function was developed to overcome such problems. This resulted in a nest of three algorithms named Popper's razor 1, 2 and 3.[2] This approach was used here to discriminate between the 15 obsidian sources from Japan. The results are given in Table 4.

Table 4 show that there is considerable overlap between sources 2, 3, 4 and 5 (Azeria, Higashi Mochiya A, Higashi Mochiya B and Kobukazawa, all from Shinshu), which clearly form a close-knit group, with considerably higher values for F, Mn and Rb than other sources. We should remember that F and Rb are highly correlated ($r = 0.85$), so it is really only two elements that are higher than in these sources than in others.

There is also about 25% overlap between sources 9 and 10 (Sanuka and Sawajiri Bay on Kōzu Island in the Izu group). These two sources have fairly distinctive values of Mn and Rb, and low values of Ga and Pb.

Table 4 Overlaps between one source and another. The estimated number of individuals that would be closer to the centroid of another source than to that of the correct source is shown below, for 1000 individuals. This is calculated from the probability of overlap in an 18-dimensional hyperspace from Mahalanobis D^2.

Source	**1**	**2**	**3**	**4**	**5**	**6**	**7**	**8**	**9**	**10**	**11**	**12**	**13**	**14**
2	0													
3	0	0												
4	0	8	401											
5	0	244	34	165										
6	1	0	0	0	0									
7	0	0	0	0	0	2								
8	0	0	0	0	0	0	3							
9	0	0	0	0	0	0	0	0						
10	0	0	0	0	0	0	0	0	243					
11	8	0	0	0	0	0	0	0	0	0				
12	0	0	0	0	0	0	19	0	0	0	0			
13	9	0	0	0	0	0	0	0	0	0	840	0		
14	0	0	0	0	0	0	4	0	0	0	0	3	0	
15	1	0	0	0	0	0	0	0	0	0	0	2	5	36

Finally, sources 11 and 13 (Koshidake and Muta on Kyushu) are clearly extremely similar, with about 85% overlap. They have quite distinctive Rb and Sr concentrations.

Apart from these three covarying groups, which are clearly quite similar geochemically, there is little multivariate overlap between other sources, or indeed between any one of the three groups and another. This is a very satisfying result.

Canonical analysis was performed on the element data of the 15 sources. The first eigenvector extracted 86% of the total variance, the first two eigenvectors 95% and the first three 98%. Clearly, the multivariate relationships can be depicted quite satisfactorily in three dimensions. This is shown in Fig. 7.

Identification of the volcanic source of obsidian artefacts

A small sample of nine obsidian artefacts was selected to test whether their sources could be determined using the PIXE–PIGME data. The artefacts were from three different archaeological sites, all dating to the Middle Jōmon period (*c.* 5000 yrs BP), based on associated pottery finds:

A Three specimens from the Togari Ishi Museum, Parking Lot, Nagano Prefecture. Catalogue numbers JA101, JA102, JA103.

B Two specimens from the Maehara Site, Koganei city, Tokyo, Middle Jōmon, fourth pit dwelling. Catalogue numbers JG702, JG703.

C Four specimens from the Togari Ishi Site surface collection, Nagano Prefecture. Catalogue numbers JK101, JK102, JK103, JK104.

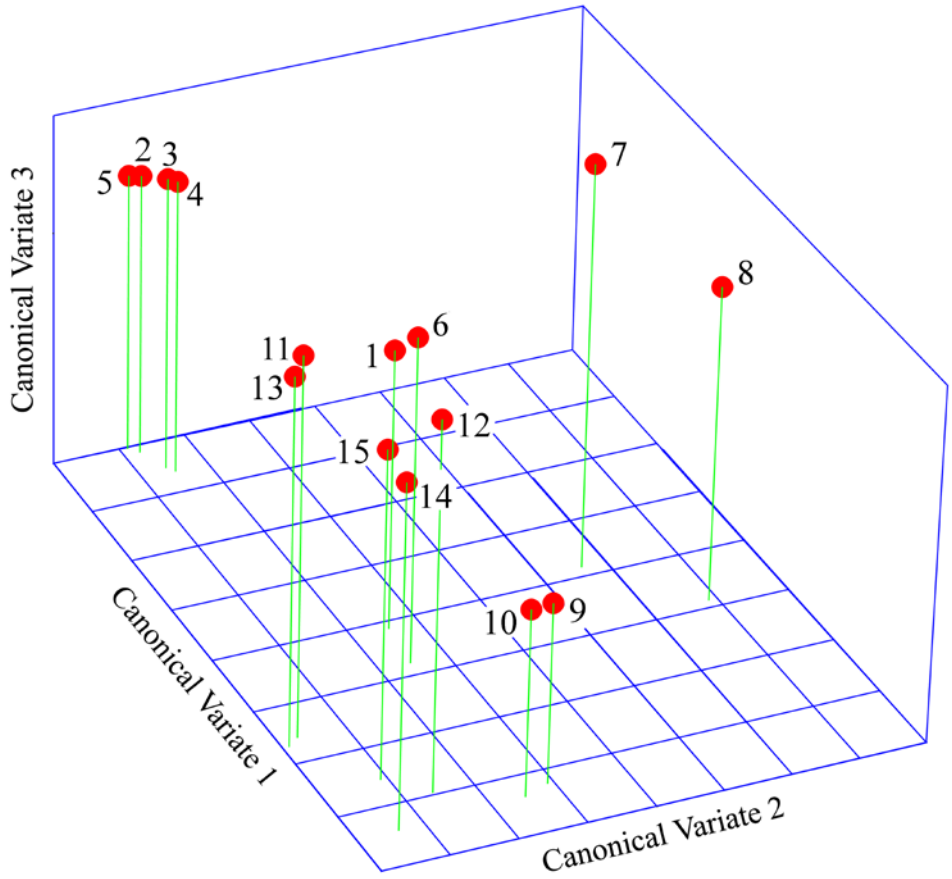

Fig. 7 Canonical analysis showing the relationship between different sources of obsidian from Japan. Three eigenvectors account for 98% of the total variance. There are three groups of sources that share significant similarity: sources 2, 3, 4 and 5; sources 9 and 10; and sources 11 and 13.

Table 5 Element concentrations for nine obsidian artefacts from Japan.

Artefact	Major elements (%)						Minor elements (μg/g)											
	Na	Al	Si	K	Ca	Fe	F	Ti	Mn	Zn	Ga	As	Pb	Rb	Sr	Y	Zr	Nb
JA101	2.34	5.92	33.59	3.31	0.50	0.77	615.0	1214.1	518.2	15.0	0.0	0.0	0.0	98.2	101.5	20.6	106.9	13.2
JA102	2.49	5.81	35.63	3.18	0.55	0.79	500.9	1202.8	504.1	19.7	0.0	0.0	0.0	88.6	101.5	24.8	117.4	8.3
JA103	2.76	6.59	39.54	3.45	0.65	0.88	571.9	1558.7	600.0	11.3	10.7	8.5	7.6	116.0	145.5	17.9	128.3	13.2
JG702	2.61	6.17	39.26	3.89	0.47	0.67	1084.1	747.4	1168.7	15.7	19.3	14.3	2.1	300.3	12.2	36.7	109.0	19.8
JG703	2.61	6.06	38.98	4.01	0.43	0.56	656.1	840.6	787.4	21.6	6.9	16.3	0.0	157.2	38.0	7.3	70.3	10.4
JK101	2.60	6.70	34.17	3.37	0.97	0.80	1016.0	883.3	1035.7	16.0	14.0	17.4	3.4	267.6	95.4	32.4	85.2	25.4
JK102	2.61	6.35	39.87	3.96	0.39	0.60	673.0	1053.2	805.7	18.8	7.1	13.3	3.4	157.1	46.0	19.4	93.9	13.5
JK103	2.59	6.11	36.60	3.56	0.38	0.58	669.0	787.2	757.3	18.2	11.9	6.1	2.6	145.1	45.1	18.2	71.9	5.9
JK104	2.57	6.20	40.30	3.95	0.47	0.56	641.7	802.6	807.7	23.4	7.8	15.8	0.5	157.8	46.8	15.9	74.5	5.3

The Mahalanobis D^2 distances were calculated between the artefact and the centroid of each of the 15 sources, divided by the effective number of dimensions in each case. If an artefact actually belongs to a particular source, the distance should be approximately 1.0.

The significance of the D^2 distance is also calculated. The results are given in Table 6.

The first three specimens – JA101, JA102, JA103, from the Togari Ishi Museum, Parking Lot site – are not significantly different from source number 7 at Mugikusa Toge, 64 km away.

Specimens JG703 from the Maehara site, and JK102 and JK103 from the surface collection at the Togari Ishi site are not significantly different from source number 1 at Hoshigatō and specimen JK104 from the same surface collection probably came from this source, but is possibly significantly different. Maehara is 118 km, and Togari Ishi 64 km, from Hoshigatō.

Specimen JG702 from Maehara is located in the overlapping regions of two sources 4 and 5, Higashi Mochiya B and Kobukazawa, and is not significantly different from either. The Maehara site is 64 km from both these sources.

Specimen JK101 cannot be allocated to any of the known sources in this study

It is interesting that artefact JG702 appears to be so similar to two of the sources, with little to separate the alternatives (2.1 and 2.2 Mahalanobis D^2 distances, respectively). In another context, when trying to locate the origin of

Table 6 Identification of the source of each artefact. Conventions for significance are: not significant (NS) = ≥ 5%; possibly significant (PS) = < 5%≥ 1%; significant (S) = < 1% ≥1%; highly significant (HS) = < 1%.

Artefact	Source	D^2	Significance	Source	D^2	Significance
JA101	7	2.2	10 NS			
JA102	7	2.1	10 NS			
JA103	7	2.5	5 NS			
JG702	4	2.1	10 NS	5	2.2	10 NS
JG703	1	2.7	5 NS			
JK101	1	7.4	0 HS			
JK102	1	2.0	10 NS			
JK103	1	2.1	10 NS			
JK104	1	3.4	1 PS			

a floating piece of obsidian (Leach *et al.* 2016), it was useful to consider the proportional difference between the element signature of an item and possible sources. Thus, the concentration of an element in the item being considered = C1, the mean concentration of a sample from the source being considered = C2, and the absolute difference (Δ1) = abs(C2–C1). The proportional difference is then ΔΔ1/C1. Such a method standardises differences, so that an element with, say, a concentration of 12µg/g will have the same weight as another element with a concentration of 2000 µg/g. The means and standard deviations of the source samples are also calculated. The standard deviations are then standardised as a proportion of the mean for each element. This permits us to visualise the variability of any one element using a standard point of reference. This is attempted in Fig. 8 using the data from artefact JG702, plotting it against the standardised data for the two alternative sources: Higashi Mochiya B (source 4) and Kobukazawa (source 5). This plot emphasises two points: these sources are very similar to each other, and the composition of the artefact is so similar to both that distinguishing between the two alternatives is not possible.

Fig. 8 (below) Comparison of artefact JG702 with two alternative sources, Higashi Mochiya B and Kobukazawa, using standardised data.

Conclusions

Japan has a large number of obsidian sources. The 15 sources studied here probably represent only about one-fifth of those known to exist. It is not known how many of the total will prove to be geochemically distinguishable from one another, but this study suggests that some sources will prove difficult to separate using element data. Many of the 15 sources studied can be clearly differentiated using the 18 elements analysed by PIXE–PIGME, but three groups of sources are extremely similar in composition. Fortunately, the sources in each of these groups are geographically close to one another, and for the purposes of identifying the movement of raw material used to make obsidian artefacts found in archaeological sites, such groupings are not significant. Other than these three groups, there is practically no multivariate overlap between the sources studied, so the task of differentiating the sources using element characteristics has been very successful.

Finally, the small number of archaeological artefacts that were analysed as a test case showed that their source could be determined with acceptable accuracy. In one case, the artefact proved to be significantly different to any of the 15 sources studied. This underlines the need to gather samples from many more volcanic sources in Japan and to characterise these in the future.

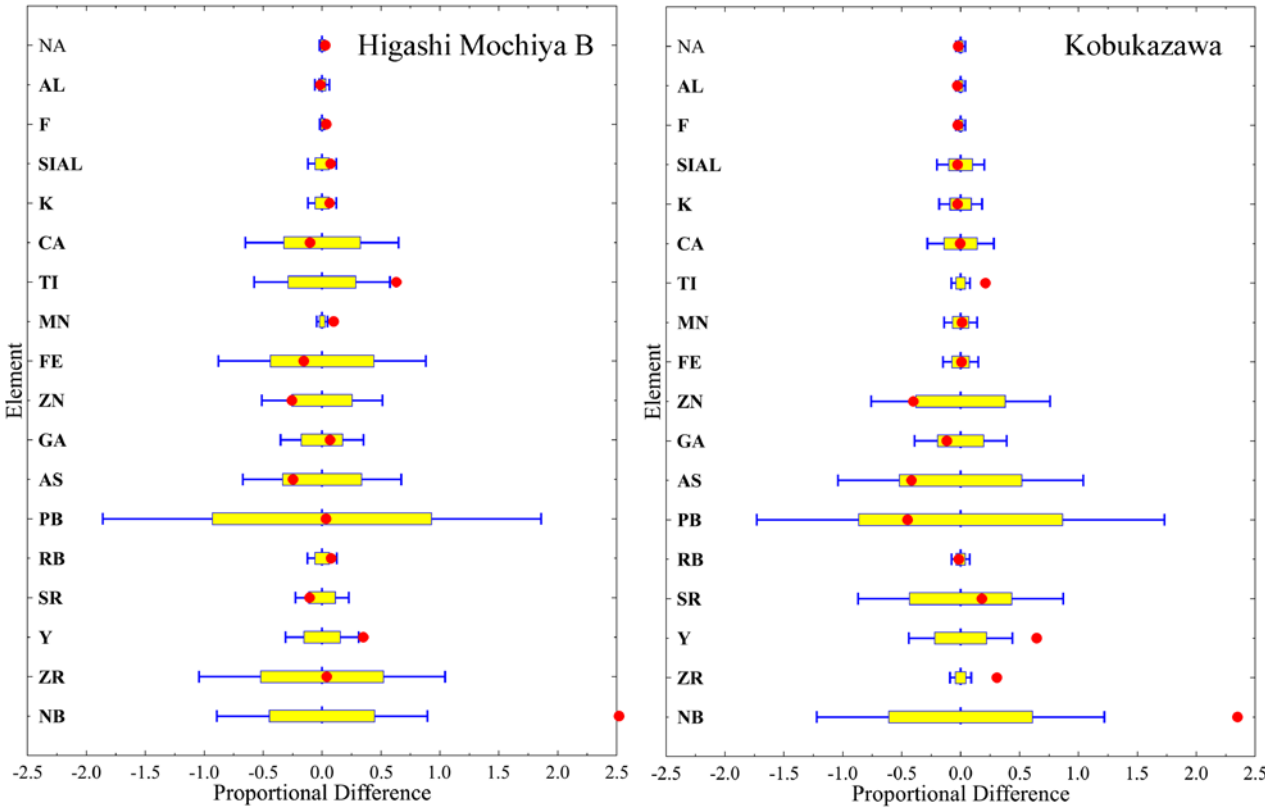

Acknowledgements

Unfortunately, one of the authors, Roger Bird, was deceased by the time this research reached publication stage. We would like to acknowledge the enthusiasm and support Dr Bird gave to the development of the obsidian-sourcing project over a long period, and the development of PIXE–PIGME as a means of assisting archaeologists in tracing the movement of raw materials in the Pacific region.

We would also like to thank the staff of Lucas Heights for the use of their 3-MeV accelerator. The samples of obsidian studied in this paper were collected by Shizuo Oda and were given to the senior author for analysis during an expedition to the Ogasawara Islands, southern Japan, in September 1989. Although the analysis was carried out shortly after that, it has taken until now to write up the results.

Notes

1 K X-rays are X-rays that arise from electron transitions in the innermost electron shell, known as the K shell.

2 These programs, together with test input and output files, may be downloaded from http://waihinga.ac.nz/foss/university-of-ngakuta/downloads/Poppers-Razor.zip.

References

Bird, J.R., Russell, L.B., Scott, M.D. and Ambrose, W.R. (1978). Obsidian characterization with elemental analysis by proton-induced gamma-ray emission. *Analytical Chemistry* 50: 2082–2084.

Clayton, E. (1982a). Sample characterization by proton induced X-ray emission analysis. *Application of Surface Science* 13: 136–158.

Clayton, E. (1982b). Some statistical techniques for provenancing artefact material: a user's view. Pp. 90–99. *In*: Ambrose, W.R. and Duerden, P. (*eds*). *Archaeometry: an Australasian perspective*. Canberra: Department of Prehistory, Australian National University. 391 pp.

Duerden, P., Cohen, D.D., Clayton, E., Bird, J.R. and Leach, B.F. (1979). Elemental analysis of thick obsidian samples by proton induced X ray emission spectrometry. *Analytical Chemistry* 51(14): 2350–2354.

Duerden, P., Bird, J.R., Scott, M.D., Clayton, E., Russell, L.H. and Cohen, D.D. (1980). PIXE–PIGME studies of artefacts. *Nuclear Instruments and Methods* 168: 447–452.

Duerden, P., Clayton, E., Bird, J.R., Ambrose, W. and Leach, B.F. (1987). Obsidian composition catalogue. Pp. 232–38. *In*: Ambrose, W.R. and Mummery, J.M.J. (*eds*). *Archaeometry: further Australasian studies*. Canberra: Department of Prehistory, Australian National University. 350 pp.

Kuzmin, Y.V. (2012). Long-distance obsidian transport in prehistoric northeast Asia. *Bulletin of the Indo-Pacific Prehistory Association* 32: 1–5.

Kuzmin, Y.V., Glascock, M.D., and Izuho, M. (2013). The geochemistry of the major sources of archaeological obsidian on Hokkaido Island (Japan): Shirataki and Oketo. *Archaeometry* 55(3): 355–369.

Leach, B.F. (1996). New Zealand and oceanic obsidians: an archaeological perspective using neutron activation analysis. *Journal of the Royal Society of New Zealand* 26(1): 79–105.

Leach, B.F. and Manly, B. (1982). Minimum Mahalanobis distance functions and lithic source characterization by multi element analysis. *New Zealand Journal of Archaeology* 4: 77–109.

Leach, B.F. and Warren, S.E. (1981). Neutron activation analysis of New Zealand and oceanic obsidians: towards a simple screening technique. Pp. 151–166 *In*: Leach, B.F. and Davidson, J.M. (*eds*). *Archaeological studies of Pacific stone resources*. British Archaeological Reports S104. Oxford: British Archaeological Reports. 237 pp.

Leach, B.F., Anderson, A.J., Sutton, D.G., Bird, J.R., Duerden, P. and Clayton, E. (1986). The origin of prehistoric obsidian artefacts from the Chatham and Kermadec islands. *New Zealand Journal of Archaeology* 8: 143–170.

Leach, B.F., Campbell, H., Eby, N., Holt, K., Regelous, M., Richards, R., and Weaver, S. (2016). Obsidian floater washed up on a beach in the Chatham Islands: geochemical composition and comparison with other volcanic glasses. *Tuhinga: Records of the Museum of New Zealand Te Papa Tongarewa* 27: 21–49

Macdonald, R. (1974). Nomenclature and petrochemistry of the peralkaline oversaturated extrusive rocks. *Bulletin Volcanologique* 38(3): 498–516.

Smith, I.E.M., Ward, G.K. and Ambrose, W.R. (1977). Geographic distribution and the characterization of volcanic glasses in Oceania. *Archaeology and Physical Anthropology in Oceania* 12(3): 173–201.